Available online at www.sciencedirect.com
SCIENCE DIRECT
Journal of Molecular Graphics and Modelling 24 (2006) 396–403
Journal of Molecular Graphics and Modelling
www.elsevier.com/locate/JMGM

Simulations of multi-directional forced unfolding of titin I27

Rudesh D. Toofanny, Philip M. Williams *

Laboratory of Biophysics and Surface Analysis, School of Pharmacy, The University of Nottingham, Nottingham NG7 2RD, UK

Received 8 March 2004; received in revised form 16 August 2005; accepted 19 September 2005
Available online 14 November 2005

Abstract

Mechanical resistance of a protein under external force is known to depend on the amino acid sequence, unfolding rate constant, topology and the direction of force applied. To assess the affect of force direction on mechanical resistance, molecular dynamics (MD) simulations of the partial unfolding of titin I27 have been carried out by applying a ramp of force between the N-terminus and the alpha-carbon of each amino acid, respectively. The results arbitrarily place the amino acids in a hierarchy in terms of the time at which an unfolding intermediate is formed. The onset of unfolding is indeed affected by force direction; directions that give maximum leverage (for the A strand to detach) unfold to the intermediate quicker than directions that give least leverage. Moreover, the change in the time taken to reach the intermediate, hence the change in mechanical resistance, can be attributed to β-strand topology. The simulations indicate that experimentally multi-directional forced unfolding could be used to reveal and study strand topology, and suggests that direction of applied force, topology and mechanical resistance are all closely related.

Keywords: Titin I27; Molecular dynamics; Protein unfolding; Dynamic force spectroscopy; Atomic force microscope

1. Introduction

Single-molecule biophysical techniques have previously been used to mechanically unfold proteins, through application of a force bias across their termini. Such techniques have revealed the dynamic force spectrum of several proteins, in particular the 27th immunoglobulin domain of the I band of titin I27 [1–4]. Experiments on single domain repeats of I27 [1] revealed the now well recognized saw tooth pattern [5] of force versus extension as the domains unfolded at forces of the order of several hundred picoNewtons. Recent studies have revealed much about the forced unfolding energy landscape for I27 and the intermediate and transition states associated with it [6–8]. Such experimental methods have been coupled with atomically detailed computational simulations that provide a molecular insight of this mechanical unfolding. The pioneering work on steered molecular dynamics (SMD) by Schulten and co-workers [9–11] revealed a relatively simple method to mimic AFM experiments of forced unfolding by fixing one terminus (akin to attaching the protein to a fixed substrate in AFM experiments) and restraining (with a harmonic restraint) the other terminus to a point in space that is moving with constant velocity and in a chosen direction.

The force exerted on the system in constant velocity SMD (SMD-CV) is expressed as:

$$f = k(v_r t - x) \tag{1}$$

where k is the stiffness of the restraint corresponding to a protein being pulled by a harmonic spring of stiffness (k). x is the initial position of the restraint point moving with constant velocity v_r. The current sub-microsecond timescale of atomistic simulations means that SMD-CV has to be undertaken with stiff constraints (circa $k = 10\, k_B T\, \text{Å}^{-2} \approx 4000$ pN nm^{-1}) and fast velocities (circa $v = 10^{10}$ nm s^{-1}) compared to those used experimentally (circa 40 pN nm^{-1} and 10^3 nm s^{-1}). Despite these limitations, SMD first predicted the presence and structure of an intermediate on the unfolding pathway of titin I27 [9], and its existence was later noted experimentally [2,7]; simulations and experiments agreed that removal of the A β-strands lead to a ∼6 Å extension of the Ig domain (Fig. 1).

Pioneering experimental investigations by [12,13] showed that the direction at which force is applied plays a significant role in the mechanical stability of ubiquitin and the E2lip3 protein, respectively. N–C linked ubiquitin chains were compared to Lys48-C linked chains through use of the AFM. It was observed that, along with sequence, topology and kinetic stability, pulling direction also dictates the

* Corresponding author. Tel.: +44 115 9515025; fax: +44 115 9515110.
E-mail address: phil.williams@nottingham.ac.uk (P.M. Williams).

1093-3263/$ – see front matter © 2005 Elsevier Inc. All rights reserved.
doi:10.1016/j.jmgm.2005.09.005

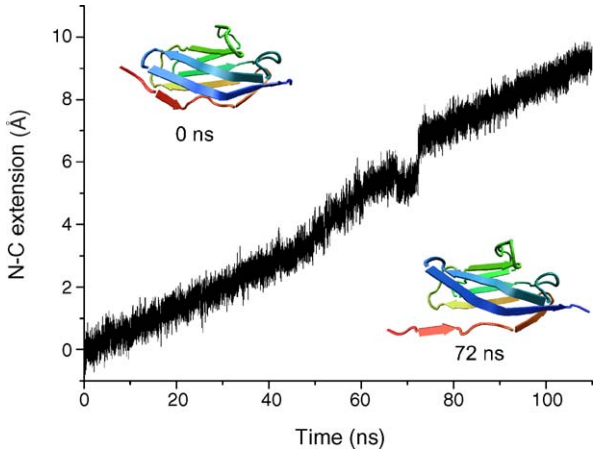

Fig. 1. Steered molecular dynamics and constant force simulations of I27 unfolding both indicate the presence of an unfolding intermediate where the A strand has separated. Shown is the extension of the N-to-C distance during a steered molecular dynamics simulation (retract velocity = 0.1 Å ns^{-1}, potential stiffness = 30 pN $Å^{-1}$, i.e. 3 pN ns^{-1}, unpublished) where the unfolding to the intermediate structure is seen after 72 ns. In the study reported here, this detachment of the A strand is taken as an indication of the onset of unfolding.

mechanical stability of a protein. Experimentally, for the E2lip3 protein, pulling in different directions was achieved by the in vivo attachment of lipoic acid to the N6-amino group of a lysine residue, which permitted the immobilization to the gold substrate by means of dithiolane ring. This elegant method allows for the application of force between the lipoylated lysine residues and the N-terminus. Unfortunately, this method does not allow for all other residues to be studied as the mutations to lysine may alter both the stability and unfolding pathway of the protein. In simulations, however, such immobilization issues are not a problem and hence the full range of directions can be observed through force application between every amino acid residue and the N-terminus.

Problematically, current modelling techniques do not allow for fully atomically detailed simulations to be carried out across the experimental timescale. The nanosecond timescale of fully explicit molecular simulations is far shorter than the natural characteristic kinetic prefactor [14] of most structural transitions in large macromolecular systems such as in protein folding. Hence, mechanical unfolding in silico induced by high force loading ($kv = 40$ pN ps^{-1}), often ∼10 orders of magnitude higher in rate than the experimental technique, does not compare to the natural event. With kinetic prefactors for protein unfolding estimated at approximately 10^6 s^{-1} ([15], unpublished), the unfolding that is observed in these rapid timescale and high force simulations are not representative of the thermal unfolding which is observed in AFM. Interestingly, the high force loading and rapid timescale simulations of [9] were able to predict the structure of an unfolding intermediate that was experimentally noted [2]. Further SMD simulations suggested the key role of water in characterizing the unfolding process of I27 [10,11]. A number of other simulations on titin I27 unfolding, including models which use an implicit solvent representation of water (as we use in this study) [6,8] and course grained models [16] have revealed the same intermediate structure despite the apparent gap between the experimental and simulation timescale and lack of molecular complexity. It is unclear whether such high force and rapid timescale simulations of protein unfolding can be used to predict unfolding intermediates in proteins that are not as mechanically stable as titin I27. However, for I27, there is correlation between simulation and experiment in the presence and structure of the intermediate hence, high force and rapid timescale simulations can be assumed to representative (at least qualitatively) of experimental forced unfolding. Although unfolding is a probabilistic event occurring on timescales far beyond most molecular dynamics simulations, the fact that single MD calculations support experimental findings implies that, for I27 at least, the thermal stochastic unfolding pathway and the MD-forced unfolding pathway are initially similar. Whilst maybe fortuitous, this correlation enables us here to use few, often single MD trajectories to estimate relative kinetic stability for I27. Critically here also, unfolding simulations of multidirectional force carried out in [12,13], showed results which were in qualitative agreement with the experimental data for proteins other than I27. We stress, however, that the methodology presented here may only be applicable to I27.

In full unfolding of I27 when stressed N–C, the A strand detaches from the B strand (leading to population of the intermediate structure) followed by the detachment of the A′ from the G strand, which then leads to full unfolding [2]. Hence, the event of the A detaching from the B strand is an indicator for the onset of unfolding. We note that when stressed in different directions A strand detachment may not precede unfolding. However, as here we are always applying force to the N-terminus we assume the A strand will detach. The onset of unfolding can be observed relative to the time to the unfolding event over 200 ps as a ratio. This also gives our measure of mechanical stability for each residue and pulling direction: a residue/direction with a value of 1 is more mechanically stable than a residue/direction with a value of 0.5. Since we are operating out of the thermal driven regime, and using implicit solvent, absolute values of force and time cannot be easily compared with experimental data.

2. Methods

MD simulations were performed using MOIL [17], modified to incorporate several methods of force application including a ‘‘ramp of force’’ protocol used here. The energy function used within MOIL is a combination of AMBER [18] and OPLS [19] force fields. In these simulations, studying how mechanical force is spread across a protein, a continuum representation (Generalized Born) [20,21] of the solvent was employed to decrease computational overhead. Pulling simulations were performed in batch on a 40-processor Sun Microsystems Ultra80/Myricom Myrinet cluster running Solaris 5.8 and Sun Grid Engine 5.3. Software was compiled using Sun Forte Developer 7 FORTRAN 95 version 7.0.

The I27 Ig domain, entry 1TIT [22] from the protein databank, was minimised within MOIL and heated to 298 K

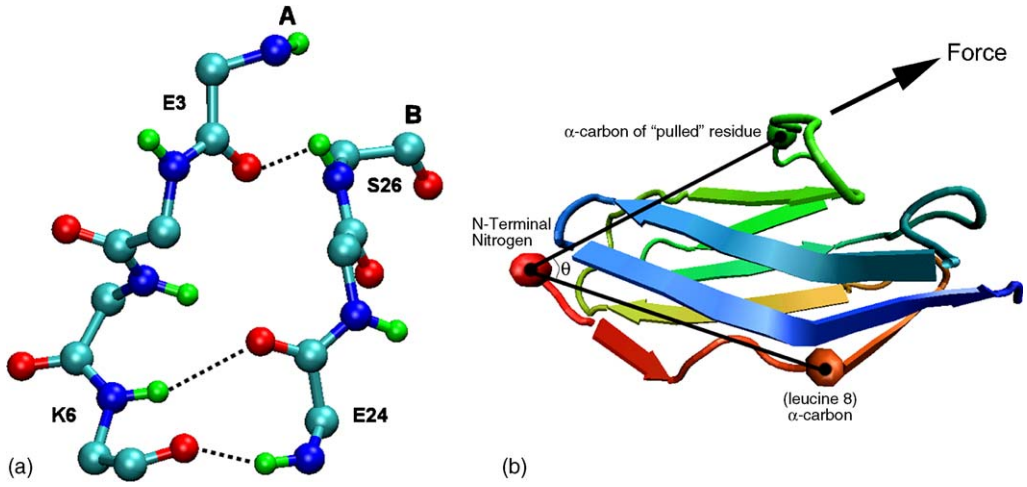

Fig. 2. (a) Snapshot of the hydrogen bond interactions between A and B β-strand backbone atoms at 0 ns. The onset of unfolding was determined if the separation of the E24:H and K6:O interaction exceeded 3 Å. Oxygen is drawn in red, hydrogen in green, nitrogen in dark blue, carbon in light blue and a dashed black line shows H-bonds. (b) Native structure of titin I27 annotated with lines to show how the angle of force was calculated. The angle measured was that made between the N-terminal nitrogen, the α-carbon of Leucine 8 and the respective residue being pulled.

over 200 ps, and then kept at this temperature for a further 1 ns; RMSD from the native was ∼1.5 Å on average during the equilibration state (of course, on the nano-second timescale there will be little change in conformation). Unfolding was induced by applying a ramp of force (4 pN ps^{-1}) between the nitrogen of the N-terminal leucine and, in turn, the alpha-carbon of each amino acid (Fig. 2b). The pulling direction is defined by the vector connecting the N-terminal nitrogen and the alpha-carbon of the ''pulled'' residue. A total of 89 simulations, each of 200 ps, were performed. Structures were saved every 0.2 ps for analysis.

I27 is known to unfold under force via an intermediate in which the A strand is detached, and in detailed molecular dynamics simulations in which force is applied between then N and C termini this event is seen prior to the unfolding event (Fig. 1). For this study, in which we were studying how the topological application of force affects the unfolding rate, we use this detachment event as an indication of the onset of unfolding. The A strand was determined to be detached from the protein if the distance between the final hydrogen bond of the A strand and B strand (K6:O and E24:H) increased above 3 Å and the distance continued to increase (Fig. 2a). The time at which this event occurred was recorded. Instances in which the extension went above 3 Å and then below were discounted and the simulation continued.

The mechanical resistance to unfolding is measured as the ratio of time it took to detach the A from the B strand to the total simulation time of 200 ps. If the A strand detached from the B strand after only 50 ps, then this would correspond to a mechanical resistance of 0.25. This measurement is used, as it is not possible to directly compare the absolute forces and times predicted by these simulations to experiment.

As the detachment of the A strand from the B strand was our indicator for the onset of unfolding, a number of simulations were extended beyond the 200 ps time to confirm that unfolding beyond the intermediate ensued in the same order as predicted by unfolding to the intermediate.

To ensure that the unfolding trend was independent of pulling force a number of pulling directions were also repeated using different ramp of force values: 10, 50, 100 and 1000 pN ps^{-1}.

3. Results

The results of the forced unfolding by applying a ramp of force between the N-terminus and each individual amino acid of I27 are summarised in Fig. 3. The A strand was found to detach in 57 of the 89 simulations run. As expected, application of force to the alpha-carbons of the residues

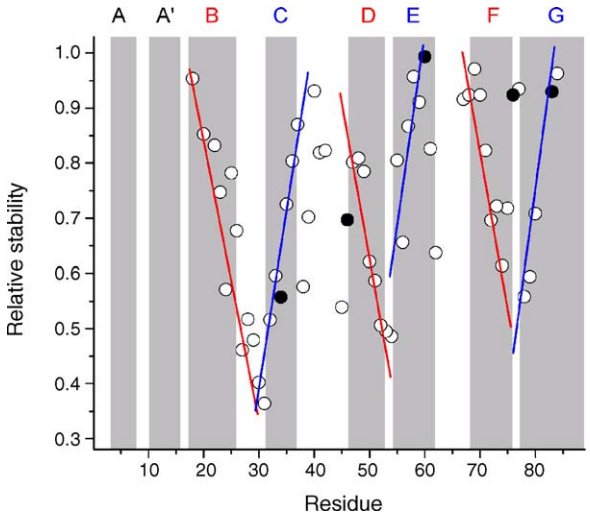

Fig. 3. The relative stability of the I27 domain to unfolding under an external force follows the strand topology. The stability is defined as the fraction of the 200 ps simulation before detachment of the A strand. The topology is indicated by the shaded regions, and lines added indicate the general trend. Solid circles as those residues studied for extended unfolding (see Fig. 4a).

within the A and A′ strands did not cause detachment. Observed times of detachment of the A strand, according to the criteria described in the previous section, for those 57 amino acids were between 73 and 199 ps, and our measure of mechanical stability scaled between 0.37 and 1.0. The mechanical stability generally follows the strand topology, with the red and blue lines added to guide the eye. The time taken for the A strand to detach decreases as the residues of the B strand get nearer to the N-terminus. For the C strand the time taken increases moving away from the N-terminus, for the D strand the time decreases, E strand increases, F strand decreases and G strand increases. At the inter-strand loops, between C and D, E and F, and F and G, this pattern is not followed most likely because these are flexible regions of the protein relative to the strand regions, which are restrained by hydrogen bonding.

Simulations that were continued until complete unfolding revealed the topological dependence on force to unfolding beyond the intermediate state (Fig. 4a). Complete unfolding was deemed to have commenced when the radius of gyration of the protein increased by 16 Å, the value of the intermediate. The resistance to complete unfolding for pulled residues (in order 60, 83, 76, 46 and 34, Fig. 4a) followed the same hierarchy as the resistance to formation of the intermediate (filled circles, Fig. 3).

The results of unfolding simulations using different ramps of force on residues 27, 31, 34, 46, 60, 76 and 83 are shown in Fig. 4b. The mechanical resistance for force on these residues under loading rates of 10, 50, 100 and 1000 pN ps^{-1} are plotted against the mechanical resistance measured under the 4 pN ps^{-1} used in the full study. A perfect correlation would indicate no dependence of rate on the measured values. A drop in value along the plot, such as for residue 46 stressed at 100 pN ps^{-1}, indicates a change in the order of measured mechanical stability.

The angle at which the force is applied θ_f relative to the N-terminal nitrogen the alpha-carbon of leucine 8 (last inter-strand loop residue between A and A′) and the alpha-carbon of the respective amino acid was also measured (Figs. 2b and 5a).

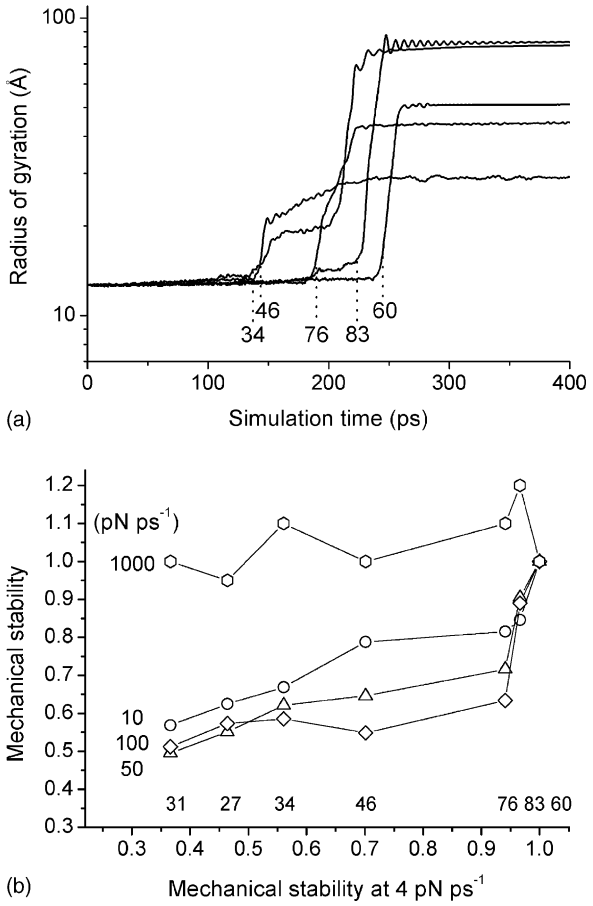

Fig. 4. (a) Complete unfolding of I27 was studied by monitoring the radius of gyration as a function of time. The protein was deemed to have commenced complete unfolding where the radius exceeded 16 Å. The order of pulled residues for complete unfolding was 34, 46, 76, 83 and 60 (quickest to slowest). These residues are shown as solid circles in Fig. 3. (b) The plot of measured relative mechanical stability derived from simulations using 10, 50, 100 and 1000 pN ps^{-1} ramps of force vs. those measured at 4 pN ps^{-1} reveals the same hierarchy of stability when measured at 4, 10 and 50 pN ps^{-1}. At 100 pN ps^{-1} residue 46 is mischaracterized in relative stability. At 1000 pN ps^{-1} no discrimination could be made.

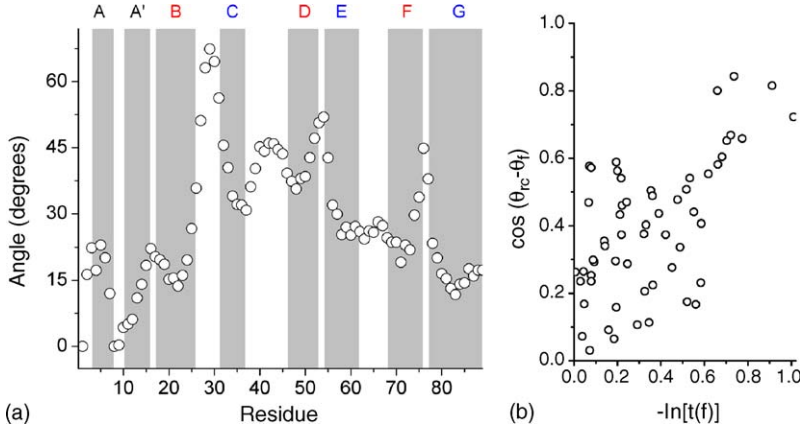

Fig. 5. (a) The angle θ_f at which force was applied in the simulation correlates with the strand topology. Comparison with the time to unfold (Fig. 3) indicates that the angle represents the extend of "leverage" on the A strand, where a high angle (residue 30 for instance) leads to fast unfolding, and vice versa. The unfolding coordinate is therefore approximately orthogonal to the N-to-C axis. (b) A plot of $\cos(\theta_{rc} - \theta_f)$ against $-\ln$[relative stability] (see text) shows a reasonable correlation when $\theta_{rc} = 90°$.

Generally, as the angle of force applied increased, corresponding to a greater mechanical leverage, the time for the unfolding event to occur decreased (compare Figs. 3 and 5a). For residues within the β-strand regions the largest angle is ∼56° for residue 27, which corresponds to the quickest time to the unfolding event of the β-strand residues. At the largest angle (∼68°), on the inter-strand region between B and C (residue 29), the time to the unfolding event is close to the fastest. The residue when pulled provided the least mechanical resistance, 31, is also in the inter-strand region between B and C.

4. Discussion

Mechanical unfolding of proteins, in particular titin I27, has previously been observed by application of a force across their termini [1–4]. More recently experimental methods to study the effect of force direction on the unfolding of globular proteins have been observed [12,13]. Experimentally the immobilization of specific residues can limit the direction in which a force can be applied. In MD simulations, however, all residues are accessible to force application. Our computational method to assess the effect of direction of force on unfolding, in terms of when a specific event occurs when a ramp of force is applied between the respective alpha-carbon of each amino acid, in turn, and the nitrogen on the N-terminal leucine, gave results that appear reasonable from a mechanical argument. The result of this multidirectional application of force shows that the direction of force does indeed affect the occurrence of the unfolding event. Fig. 3 shows clearly that moving down the amino acid residues of the B strand from the N-terminus that the time taken for the unfolding event to occur decreases and then increases as move up the C strand, and so on. The angle at which the force is applied relative to the position of the N-terminal nitrogen, the alpha-carbon of the last residue of the inter-strand loop between A and A′ (leucine 8) and the residue being pulled (Fig. 2b) also correspond with the time taken (Fig. 5a). The direction of force applied effects the mechanical stability and the mechanical resistance appears to be derived from topology, as postulated previously. Thus, mechanical resistance of a protein is dependent on chain sequence, structure, topology, and kinetic stability and, moreover, the direction of force applied.

In these somewhat crude simulations, with the rapid timescale (ps as opposed experimental ms), high force applied and implicit solvent, it is observed that the intermediate structure (where the A strand has detached) is present (Fig. 1) as indicated experimentally [2,7]. These simulations operate in a regime of high force and the unfolding events are not due to thermal energy, solely force applied. Despite this, the well-characterised intermediate is observed which pays testament to the mechanical stability of the intermediate and unfolding energy landscape of I27, which is more than likely the reason why the rapid timescale and high force SMD simulations were first to observe this [9].

The simulations extended beyond formation of the unfolding intermediate indicate that our 200 ps simulations, which use the detachment of the A strand from the B strand as an indicator of the onset of unfolding, are indeed representative of the relative mechanical stability. The order of mechanical stability to complete unfolding of the chosen residues is the same as for intermediate formation (Fig. 4a).

As expected, increasing the ramp of force in the simulations did alter the time to detachment of the A strand. Importantly, the relative mechanical stability measured was the same for simulations performed at 4, 10 and 50 pN ps^{-1}. At 100 pN ps^{-1} 1 (25 times the rate used in the full study) one residue (46) was misplaced in stability. We note that this residue in strand D is adjacent to a flexible loop where the force behaviour is varied (Fig. 3). At 1000 pN ps^{-1}, all structures unfolded to the intermediate within a few picoseconds precluding the accurate determination of the relative mechanical stability. Whilst it is true that more representative simulations would have emerged from using longer periods and lower forces, these results indicate that the 200 ps simulations performed reflected the order of relative mechanical stability.

It is interesting to note that whilst the relative mechanical stability can be determined using a number of fixed loading rates up to 50 pN ps^{-1}, there appears to be a non-monotonic dependence on the relative stability with loading rate. In Fig. 4b, the stabilities measured at 10 pN ps^{-1} appear consistently higher than those measured at 50 and 100 pN ps^{-1}, 1, which themselves change in order for different residues. This behaviour may be an artefact of limited sampling, although the fact that the same ordering of relative stability is retrieved for all but the very highest rates suggests otherwise.

The relative stability data reveals a fingerprint of the immunoglobulin like domain, with our measure of relative resistance to unfolding (Fig. 3) following the topology of the protein. The correlation between the mechanical strength and the geometry of the protein, and topology, allows us to make a simple prediction of the experimental behaviour. Under an external force potential, applied for example by an atomic force microscope, the unfolding rate is increased as force lowers the magnitude of the unfolding transition state energy relative to the native state. Alternatively, one can consider force as stabilizing the unfolded state and destabilizing the transition state and the folded state more so. The net effect of force is a reduction in the activation energy required to unfold and a resulting exponential increase in the unfolding rate with linear increases in force. This exponential effect of force on the unfolding kinetics, due to the reduction in activation energy, is related to both the amount of force applied and the distance along the unfolding coordinate that the force is applied. Neglecting for simplicity any force-induced movement of the transition state the unfolding rate under force can be expressed in terms of the force-free unfolding rate k_u^0, the force applied F, the displacement of the transition state x_u, and the angle $(\theta_{rc} - \theta_f)$ between the unfolding coordinate and the direction at which the force is applied off the unfolding coordinate, as:

$$k_u(f) \approx k_u^0 \exp\left(\frac{F x_u \cos(\theta_{rc} - \theta_f)}{k_B T}\right) \quad (2)$$

To estimate the direction of the unfolding coordinate θ_{rc} relative to the direction at which force was applied we assumed from

Eq. (2) that the time to unfold would be inversely proportional to the projection of force along the unfolding coordinate, as:

$$\cos(\theta_{rc} - \theta_f) \propto -\ln[t(f)] \quad (3)$$

Eqs. (2) and (3) are valid for the experimental regime with a number of qualifications such as the force being quasi-static on the time scale of the kinetic prefactor (experimental loading rates of less than 10^4 pN s^{-1} and unfolding prefactors faster than 10^6 s^{-1} means that force changes by less than 0.01 pN within the time of each unfolding attempt) and a deep folding potential (with minimal barrier movement under force). In our simulations, we measured the ease at which force removes the A strand depending on the direction at which force was applied. By assuming that the simulations 'pull' the system over the same barrier to A strand removal that the it would thermally diffuse over, we can correlate the simulation times and angles of force to approximate the angle at which the reaction coordinate makes with the $K1_N$–$K8_{C\alpha}$ axis from which the angles were measured. Fig. 4b shows the correlation of Eq. (3) using a reaction coordinate angle θ_{rc} of 90°.

Since here we have predicted the ease at which unfolding to the I27 intermediate occurs (as this is a well defined event), and experimentally it is the unfolding from the intermediate that is measured (which is difficult to locate in simulations without supporting experimental data such as phi-values), we have to assume that the angular dependence seen in the simulations is reflected in the experiment. There is little reason to doubt this assumption, and encouragingly the experimental results on ubiquitin support the case where the apparent location of the single transition state shifts with the direction of force [12]. The simulations extended to complete unfolding also produced the same mechanical hierarchy (Fig. 3 solid circles and Fig. 4a). However, the θ_{rc} of the major unfolding barrier will almost certainly differ from that of the A strand barrier measured.

Using a simple analytical approximation of the most probable unfolding force:

$$f^* \approx \frac{k_B T}{x_u \cos(\theta_{rc} - \theta_f)} \ln\left(\frac{r'_f}{k_u^0} \frac{x_u \cos(\theta_{rc} - \theta_f)}{k_B T}\right) \quad (4)$$

where the complex loading dynamics of the system are encompassed in an effective force loading rate r'_f, we can predict, using k_u^0 and $x_u \cos(\theta_{rc} - \theta_{N-C})$, the directional dependence of the unfolding force seen in AFM experiments. Fig. 6 shows this prediction using three values of θ_{rc} of 60° (green), 75° (blue) and 90° (red) and $x_u \cos(\theta_{rc} - 17) = 2.9$ Å, $k_u^0 = 2 \times 10^{-4}$ s^{-1}, and $r'_f = 1600$ pN s^{-1}. Again, force values are relative and although we give absolute values in picoNewtons these are provided to indicate only the scale of the forces predicted. The unfolding forces are predicted to reflect the strand topology with the absolute value of the unfolding coordinate θ_{rc} modulating the response.

We predict that the relative mechanical stability of I27 under directional force is greatest for stresses parallel to the N-to-C axis; this finding relates directly to the natural role of the protein. Titin (also known as connectin) is found in muscle connecting the thick and thin filaments via connections at the

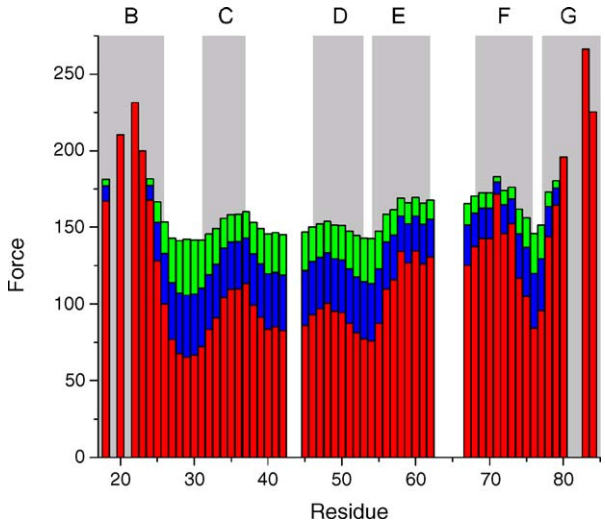

Fig. 6. Changing the direction at which force is applied will change the mechanical stability of the protein. Scaled to the value measured experimentally when pulled in the AFM at 1000 nm s^{-1}, we predict the unfolding force for I27 will follow the strand topology. The domain is most stable under forces parallel to the N-to-C axis. The results are shown for three difference reaction coordinate vectors (green 60°; blue 75°; and red 90°).

Z-disc and *M*-line, and as a tandem repeat of immunoglobulin domains is several microns in length. Fig. 6 suggests that a repeat of domains with the N and C termini anything other than diagonally opposed would be weaker and this topology represents that of maximum strength. But if titin's role is to act only as a passive spring to maintain symmetry of the two I-bands and prevent overstretching of the muscle, why does nature use tandem repeats of many folded domains and not just a far more easily made random coil of much less amino-acids? Considering each domain of titin to be rigid, the stiffness $\kappa_s(F)$ of a tandem repeat of domains approximates to a freely-jointed chain (FJC) and held at a high force F its stiffness is:

$$\kappa_s(F) \approx \frac{k_B T}{bL}\left(\frac{bF}{k_B T}\right)^2 \quad (5)$$

where b is the length of each segment and L the contour length of the chain [23]. With the number of amino acids required to fold into a globular domain scaling approximately with the cube of domain's N-to-C distance, the stiffness of a 1 μm FJC polymer held at a physiological force of 20 pN as a function of the number of amino acids required can be plotted (scaled in this case to the 4.5 nm size for 89 amino acids of I27) and is shown in Fig. 7. It can be seen that the rigidity initially rapidly increases as each domain increases in size. However, the number of amino acids required to form stiffer chains of ever larger domains becomes prohibitively great. Of course, titin is not just comprised of Ig domains but has many components, such as the flexible PEVK regions, which contribute to the mechanical properties, but this simple analysis suggests that the 89 amino acid Ig domain offers good mechanical properties for a fixed budget of complexity.

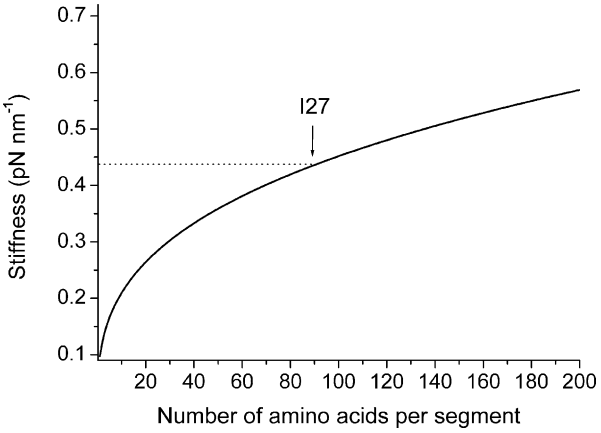

Fig. 7. Tandem repeats of protein domains, such as those seen in titin, are predicted to behave as freely jointed chains. The stiffness of a 1 μm chain held at a physiological force of 20 pN is predicted to increase with the size of the domains. Assuming the number of residues required to form a domain scales with the third power of the size, a compromise in strength and complexity is noted for domain sizes comparable to I27.

Finally, if one could measure the directional force dependence through the use of AFM for other force techniques, it could be possible to determine structure for beta sheet proteins. Given only sequence information, unfolding experiments by pulling on each residue of the protein would give a rupture force *vs.* residue plot which follows the 'zigzag' pattern observed here. Since the longest sheet length is of order root three of the total sequence length, the positions and topology of the beta sheets could be predicted from such data. Before such experiments can be conducted and the full topology of a protein explored, however, limitations of selecting and immobilising individual residues to the AFM tip will have to be overcome.

5. Conclusion

We have presented a set of MD simulations (quick and high force) that assess the affect of pulling direction and topology on unfolding rate of titin I27. We find that the β-strand topology of titin I27 can be mapped out and that, indeed, pulling direction and topology affect the unfolding rate whereby moving up and down the β-strands unfolding rate decreases and increases. This simple method appears to be a good pre-empt to experimental unfolding of titin I27 that assess the affect of pulling direction, and the results hint at Nature's elegant use of classical and statistical mechanics.

Acknowledgments

We thank Sheena Radford and Alastair Smith from the University of Leeds for discussions and the inspiration for this work, and Jane Clarke from Cambridge University for many valuable lessons and debates on I27 and protein (un)folding. R.D.T. thanks the EPSRC and the University of Nottingham for funding. P.M.W. is an EPSRC Advanced Research Fellow. Part of this work and manuscript preparation was undertaken by P.M.W. whilst attending an Isaac Newton Institute for Mathematical Sciences programme on Statistical Mechanics of Molecular and Cellular Biological Systems running January to July 2004.

References

[1] M. Carrion-Vazquez, P.E. Marszalek, A.F. Oberhauser, J.M. Fernandez, Atomic force microscopy captures length phenotypes in single proteins, Proc. Natl. Acad. Sci. U.S.A. 96 (1999) 11288–11292.
[2] P.E. Marszalek, H. Lu, H. Li, M. Carrion-Vasquez, A.F. Oberhauser, K. Schukten, J.M. Fernandez, Mechanical unfolding intermediates in titin modules, Nature 402 (1999) 100–103.
[3] H. Li, M. Carrion-Vazquez, A.F. Oberhauser, P.E. Marszalek, J.M. Fernandez, Point mutations alter the mechanical stability of immunoglobulin modules, Nat. Struct. Biol. 7 (2000) 1117–1120.
[4] D.J. Brockwell, G.S. Beddard, J. Clarkson, R.C. Zinober, A.W. Blake, J. Trinick, P.D. Olmsted, D.A. Smith, S.E. Radford, The effect of core destabilization on the mechanical resistance of I27, Biophys. J. 83 (2002) 58–72.
[5] M. Rief, M. Gautel, F. Oesterhelt, J.M. Fernandez, H.E. Gaub, Reversible unfolding by individual titin immunogloblin domains by AFM, Science 276 (1997) 1109–1112.
[6] S.B. Fowler, R.B. Best, J.L. Toca-Herrera, T.J. Rutherford, A. Steward, E. Paci, M. Karplus, J. Clarke, Mechanical unfolding of a titin Ig domain: structure of unfolding intermediate revealed by combining AFM, molecular dynamics simulations, NMR and protein engineering, J. Mol. Biol. 322 (2002) 841–849.
[7] P.M. Williams, S.B. Fowler, R.B. Best, J.L. Toca-Herrera, K.A. Scott, A. Steward, J. Clarke, Hidden complexity in the mechanical properties of titin, Nature 422 (2003) 446–449.
[8] R.B. Best, S.B. Fowler, J.L. Herrera, A. Steward, E. Paci, J. Clarke, Mechanical unfolding of a titin Ig domain: structure of transition state revealed by combining atomic force microscopy, protein engineering and molecular dynamics simulations, J. Mol. Biol. 330 (2003) 867–877.
[9] H. Lu, B. Isralewitz, A. Krammer, V. Vogel, K. Schulten, Unfolding of titin immunoglobulin domains by steered molecular dynamic simulations, Biophys. J. 75 (1998) 662–671.
[10] H. Lu, K. Schulten, The key events in force induced unfolding of titin's immunoglobulin domains, Biophys. J. 79 (2000) 51–65.
[11] M. Gao, H. Lu, K. Schulten, Simulated refolding of stretched titin immunoglobulin domains, Biophys. J. 81 (2001) 2268–2277.
[12] M. Carrion-Vazquez, H. Li, H. Lu, P.E. Marszalek, A.F. Oberhauser, J.M. Fernandez, The mechanical stability of ubiquitin is linkage dependent, Nat. Struct. Biol. 10 (2003) 738–743.
[13] D.J. Brockwell, E. Paci, R.C. Zinober, G.S. Beddard, P.D. Olmsted, D.A. Smith, R.N. Perham, S.E. Radford, Pulling geometry defines the mechanical resistance of a beta-sheet protein, Nat. Struct. Biol. 9 (2003) 731–737.
[14] W.Y. Yang, M. Gruebele, Folding at the speed limit, Nature 423 (2003) 193–197.
[15] P.M. Williams, R.D. Toofanny, K.A. Scott, J. Clarke, unpublished.
[16] M. Cieplak, T.X. Hoang, M.O. Robbins, Folding and stretching in a Go-like model of titin, Proteins 49 (2002) 114–124.
[17] R. Elber, A. Roitberg, C. Simmerling, R. Goldstein, H. Li, G. Verkihvker, C. Keasar, J. Zhang, A. Ulitsky, MOIL: a program for simulations of macromolecules, Comput. Phys. Commun. 91 (1995) 159–189.
[18] S.J. Weiner, P.A. Kollman, D.A. Case, U.C. Singh, C. Ghio, G. Alagons, S. Profeta Jr., P. Weiner, A new force field for molecular mechanical simulation of nucleic acids and proteins, J. Am. Chem. Soc. 106 (1984) 765–784.
[19] W.L. Jorgensen, J. Tirad-Rives, The OPLS potential functions for proteins. Energy minimization for crystals of cyclic peptides and crambin, J. Am. Chem. Soc. 110 (1998) 1657–1666.

[20] G.D. Hawkins, C.J. Cramer, D.G. Truhlar, Pairwise solute screening of solute charges from a dielectric medium, Chem. Phys. Lett. 246 (1995) 122–129.
[21] V. Tsui, D.A. Case, Theory and applications of the generalized Born solvation model in macromolecular simulations, Biopolymers 56 (2000) 275–291.
[22] S. Improta, A.S. Politou, A. Pastore, Immunoglobulin-like modules from titin I-band: extensible components of muscle elasticity, Structure 4 (1996) 323–337.
[23] P.M. Williams, E. Evans, in: H. Flyvbjerg, F. Julicher, P. Ormos, F. David (Eds.), Les Houches Session LXXV, Physics of Bio-molecules and Cells, Springer–Verlag, New York, 2002, pp. 187–204.